

Rigorous Test of the Forward Dispersion Relation and Determination of πN Low-Energy Parameters

T. N. Pham and Tran N. Truong

*Centre de Physique Théorique, de l'Ecole Polytechnique, 17, rue Descartes, 75230 Paris Cedex 05, France**

(Received 26 March 1973)

General and rigorous methods for testing ordinary and average πN forward-dispersion relations using experimental data at finite energy are given. Using the total cross-section data up to 60 GeV, it is found that the energy variation of the real part of the symmetric forward amplitude is compatible with experimental data in the 8–20-GeV region. The magnitude of the real part in this energy range cannot be strictly tested without total cross-section data from the National Accelerator Laboratory. An average upper bound for the sum of $\pi^+ p$ and $\pi^- p$ total cross sections in the range of 60–500 GeV is given, which can be used as a rigorous test of the dispersion relation. General and rigorous methods are also given for the determination of low-energy parameters. It is shown that the πN coupling constant can be determined in principle to better than 1%. Low-energy data with great precision are required from pion factories for an accurate determination of all πN low-energy parameters.

I. INTRODUCTION

One of a few physically interesting results in particle physics which can be derived from axiomatic field theory is the forward dispersion relation. It is of great importance therefore to confront the dispersion relation with experiments. However, it is difficult to test the dispersion relation for the following reasons:

- (i) The total cross sections must be known at all energies from the threshold energy up to infinity.
- (ii) An assumption of a smooth behavior for the total cross sections is required in carrying out the principal-part integration.

The second point can be minimized by considering instead an averaged forward amplitude over an energy interval. The result is essentially the same as that obtained from the ordinary dispersion relations, assuming smoothness for the total cross sections. Depending on the situation, in this paper we shall use both the ordinary and average dispersion relations.

The first point is much more difficult to handle. From the axiomatic field theory we know very little about the high-energy behavior of the forward scattering amplitude. Although the Froissart-Martin upper bound¹ for the total cross section, i.e., as $s \rightarrow \infty$

$$\sigma_{\text{tot}} \leq \frac{\pi}{\mu^2} \ln^2(s/s_0),$$

is reasonably good, it tells us neither at what energy this bound becomes effective nor what the scale in the $\ln^2 s$ term is. The lower bound is much worse; all we know is that

$$\sigma_{\text{tot}} > \frac{C}{s^2 \ln^2 s}$$

for $s \rightarrow \infty$.

For the above reasons, we cannot use these bounds directly to analyze the dispersion relation. The usual method of testing the dispersion relation consists of using the experimental data for the total cross sections up to the maximum available energy and of extrapolating the total cross sections to infinite energy by some model, e.g., the Regge-pole model. Judging from the published results² obtained with wildly different high-energy assumptions for the total cross sections and with the same input for the real part of the forward amplitude, we can conclude that these results reflect more a test of the acceptable assumptions on the asymptotic cross sections than a test of the dispersion relation. This will become clear as discussed below.

In this article we shall not make any assumption on the total cross section beyond the maximum energy which can be attained by accelerators. The Froissart-Martin bound is used only to establish the maximum number of subtractions needed. Making use of positivity of the total cross sections, we give obvious but strict inequalities which can be used to test the dispersion relation without any ambiguity. The method used is quite general and is suitable for planning future experiments at the Serpukhov and National Accelerator Laboratory (NAL) accelerators.

The paper is organized as follows. In Sec. II we give different methods for testing the $\pi^+ p$ forward dispersion relation at high energy. Starting with the dispersion relation for $\text{Re} f^\pm(\omega)$ we show that, for the case in which the real part of $f^\pm(\omega)$ is measured at energies which are small compared to the maximum energies at which the $\pi^+ p$ total cross sections are available, strict lower and upper bounds for the high-energy dispersion integral (to be defined below) at one energy can be obtained in

terms of that at another suitably chosen energy (i.e., tests of the energy variation of the real part). This enables us to test the dispersion relation for $f_S(\omega)$ [defined as $\frac{1}{2}f^+(\omega) + \frac{1}{2}f^-(\omega)$] or for both $f^+(\omega)$ and $f^-(\omega)$ separately by expressing the lower and upper bounds of $\text{Re}f_S(\omega)$ or $\text{Re}f^\pm(\omega)$ in terms of the finite dispersion integrals and the experimental value of $\text{Re}f^\pm(\omega)$ at another suitably chosen energy.

The above method can be applied at present to the case where $\text{Re}f^\pm(\omega)$ have been measured in the region 8–20 GeV and the $\pi^\pm p$ total cross sections measured up to 60 GeV.

We next show that a more stringent test of the dispersion relation is to compare the predicted energy-weighted average total cross sections in a high-energy interval, say, between 60 and 500 GeV, with the future experimental data to be obtained at NAL. We then extend the above analysis to the energy-weighted average amplitude taken in some energy interval to avoid the difficulty with the principal-part integration.

In Sec. III, we give a similar analysis of the dispersion relation in the low-energy region. Approximate sum rules with predetermined precisions (i.e., bounds) for $\text{Re}f_S(\omega)$ and $\text{Re}f_A(\omega)$ ($\text{Re}f_A(\omega) = \frac{1}{2}[\text{Re}f^+(\omega) - \text{Re}f^-(\omega)]$) are given in terms of finite dispersion integrals. These sum rules can be used to determine accurately the $\pi^\pm N$ s-wave scattering lengths and the pion-nucleon coupling constant.

II. TEST OF DISPERSION RELATION AT HIGH ENERGY

A. Dispersion Relation for $\pi^\pm p$ Forward Scattering Amplitude

Consider the $\pi^\pm p$ forward scattering amplitude $f^\pm(\omega)$ in the laboratory system, defined as

$$f^\pm(\omega) = \text{Re}f^\pm(\omega) + i \text{Im}f^\pm(\omega).$$

The imaginary parts $\text{Im}f^\pm(\omega)$ are related to the $\pi^\pm p$ total cross sections by the optical theorem:

$$\text{Im}f^\pm(\omega) = \frac{q}{4\pi} \sigma^\pm(\omega),$$

where ω is the energy of incident pion with momentum q [$\omega = (q^2 + \mu^2)^{1/2}$] and $\sigma^\pm(\omega)$ are $\pi^\pm p$ total cross sections in the laboratory system.

We now introduce the crossing-even and -odd amplitudes f_S and f_A , defined, respectively, as

$$f_S(\omega) = \frac{1}{2}[f^+(\omega) + f^-(\omega)],$$

$$f_A(\omega) = \frac{1}{2}[f^+(\omega) - f^-(\omega)],$$

and the corresponding quantities

$$\sigma_S(\omega) = \frac{1}{2}[\sigma^+(\omega) + \sigma^-(\omega)],$$

$$\sigma_A(\omega) = \frac{1}{2}[\sigma^+(\omega) - \sigma^-(\omega)].$$

As a consequence of analyticity, crossing symmetry, and the Froissart-Martin bound, $f^\pm(\omega)$ satisfy dispersion relations with at most two subtractions. Thus $\text{Re}f^\pm(\omega)$ are given by

$$\begin{aligned} \text{Re}f^\pm(\omega) &= \text{Re}f_S(\mu) \pm \frac{\omega}{\mu} \text{Re}f_A(\mu) \\ &\pm \frac{2f^2}{\mu^2} \left(1 - \frac{\mu^2}{4M^2}\right)^{-1} \left[\frac{q^2}{\omega \mp \mu^2/2M}\right] \\ &+ \frac{q^2}{4\pi^2} \text{P} \int_\mu^\infty \frac{d\omega'}{q'} \left[\frac{\sigma^\pm(\omega')}{\omega' - \omega} + \frac{\sigma^\mp(\omega')}{\omega' + \omega}\right], \end{aligned} \quad (1)$$

where μ is the pion mass and f^2 is the charged pion-nucleon renormalized coupling constant. $\sigma^\pm(\omega)$ are measured in units of mb, $\text{Re}f^\pm(\omega)$ and $\text{Im}f^\pm(\omega)$ in units of μ^{-1} ($1\mu^{-1} = 1.41$ fm and $1\mu^{-2} = 20$ mb).

Let us introduce the following notations [$\text{Re}f_{S,A}(\mu) = f_{S,A}(\mu)$]:

$$\begin{aligned} \text{Re}f^\pm(\omega) &= f_S(\mu) \pm \frac{\omega}{\mu} f_A(\mu) \\ &\pm \frac{2f^2}{\mu^2} \left(1 - \frac{\mu^2}{4M^2}\right)^{-1} \left[\frac{q^2}{\omega \mp (\mu^2/2M)}\right] \\ &+ J^\pm(\omega) + I^\pm(\omega), \end{aligned} \quad (2)$$

where

$$J^\pm(\omega) = \frac{q^2}{2\pi^2} \text{P} \int_\mu^N \left(\frac{\omega}{q'}\right) \frac{d\omega'}{\omega'^2 - \omega^2} \left(\sigma_S \pm \frac{\omega}{\omega'} \sigma_A\right), \quad (3a)$$

$$I^\pm(\omega) = \frac{q^2}{2\pi^2} \int_N^\infty \left(\frac{\omega'}{q'}\right) \frac{d\omega'}{\omega'^2 - \omega^2} \left(\sigma_S \pm \frac{\omega}{\omega'} \sigma_A\right). \quad (3b)$$

In terms of the crossing-even and -odd amplitudes, we have similarly

$$\begin{aligned} \text{Re}f_S(\omega) &= f_S(\mu) + \frac{f^2}{M} \left(1 - \frac{\mu^2}{4M^2}\right)^{-1} \left[\frac{q^2}{\omega^2 - (\mu^2/2M)^2}\right] \\ &+ J_S(\omega) + I_S(\omega), \end{aligned} \quad (4)$$

$$\begin{aligned} \text{Re}f_A(\omega) &= \left(\frac{\omega}{\mu}\right) \left\{ f_A(\mu) \right. \\ &+ \frac{2f^2}{\mu} \left(1 - \frac{\mu^2}{4M^2}\right)^{-1} \left[\frac{q^2}{\omega^2 - (\mu^2/2M)^2}\right] \\ &\left. + J_A(\omega) + I_A(\omega) \right\}, \end{aligned} \quad (5)$$

where

$$J_S(\omega) = \frac{q^2}{2\pi^2} \text{P} \int_0^N \frac{dq'}{\omega'^2 - \omega^2} \sigma_S(\omega'), \quad (6a)$$

$$I_S(\omega) = \frac{q^2}{2\pi^2} \int_N^\infty \frac{dq'}{\omega'^2 - \omega^2} \sigma_S(\omega'), \quad (6b)$$

$$J_A(\omega) = \frac{q^2}{2\pi^2} \text{P} \int_0^N \left(\frac{\mu}{\omega'}\right) \frac{dq'}{\omega'^2 - \omega^2} \sigma_A(\omega'), \quad (6c)$$

$$I_A(\omega) = \frac{q^2}{2\pi^2} \int_N^\infty \left(\frac{\mu}{\omega'} \right) \frac{dq'}{\omega'^2 - \omega^2} \sigma_A(\omega'), \quad (6d)$$

where $\omega < N$ and N is the maximum energy at which the data on $\sigma^\pm(\omega)$ are available (cutoff energy). $J(\omega)$ and $I(\omega)$ are called the cutoff and high-energy dispersion integrals, respectively. For convenience, we have made a change of variable $\omega' \rightarrow q' = (\omega'^2 - \mu^2)^{1/2}$ in the integrals.

Having these preliminaries out of the way, we now have to find a method for testing $\pi^\pm p$ forward dispersion relations given above.

B. Bounds on High-Energy Dispersion Integrals

1. Bounds on $I_S(\omega)$

Consider the high-energy integral $I_S(\omega)$. It is easy to see that $I_S(\omega)/q^2$ is a monotonically increasing function of the variable q . More explicitly, we have³ for $q_2 \geq q_1$

$$\frac{I_S(\omega_2)}{q_2^2} - \frac{I_S(\omega_1)}{q_1^2} = \frac{(q_2^2 - q_1^2)}{2\pi^2} \int_N^\infty \frac{\sigma_S(\omega') dq'}{(\omega'^2 - \omega_1^2)(\omega'^2 - \omega_2^2)}. \quad (7)$$

$$\frac{I^\pm(\omega_2)}{q_2} - \frac{I^\pm(\omega_1)}{q_1} = \frac{q_2 - q_1}{2\pi^2} \int_N^\infty \frac{dq'}{(\omega'^2 - \omega_1^2)(\omega'^2 - \omega_2^2)} \left[(q'^2 + q_1 q_2) \sigma_S \pm \left(\frac{q_1 + q_2}{\omega'} \right) q'^2 \sigma_A \right], \quad (10)$$

which can be written in the following form:

$$\frac{I^\pm(\omega_2)}{q_2} - \frac{I^\pm(\omega_1)}{q_1} = \frac{q_2 - q_1}{2\pi^2} \int_N^\infty \frac{dq' [(q_1 q_2 - q'^2) \sigma_S + 2q'^2 \sigma_S \pm (q'^2/\omega') (\omega_1 + \omega_2) \sigma_A]}{(\omega'^2 - \omega_1^2)(\omega'^2 - \omega_2^2)}. \quad (11)$$

For $\omega_2 \geq \omega_1$, since

$$1 - \frac{q_1(q_2 - q_1)}{N^2 - q_1^2} \leq \frac{q'^2 - q_1 q_2}{q'^2 - q_1^2} \leq 1$$

and

$$1 \leq \frac{q'^2}{q'^2 - q^2} \leq \frac{N^2}{N^2 - q^2}, \quad q = q_1, q_2$$

we obtain

$$\frac{I^\pm(\omega_2)}{q_2} - \frac{I^\pm(\omega_1)}{q_1} \geq (q_2 - q_1) \left[-\frac{I_S(\omega_2)}{q_2^2} + \frac{I^\pm(\omega_2)}{q_2} + \frac{I^\pm(\omega_1)}{q_1^2} \right] \quad (12a)$$

and

$$\frac{I^\pm(\omega_2)}{q_2} - \frac{I^\pm(\omega_1)}{q_1} \leq (q_2 - q_1) \left\{ \left(\frac{N^2}{N^2 - q_1^2} \right) \frac{I^\pm(\omega_2)}{q_2^2} + \left(\frac{N^2}{N^2 - q_2^2} \right) \frac{I^\pm(\omega_1)}{q_1^2} - \frac{I_S(\omega_2)}{q_2^2} + \left[\frac{q_1(q_2 - q_1)}{N^2 - q_1^2} \right] \frac{I_S(\omega_2)}{q_2^2} \right\}. \quad (12b)$$

Hence it follows from (12a) and (12b) that

$$I^\pm(\omega_1) \geq \left(1 - \frac{q_2^2 - q_1^2}{N^2 - q_1^2} \right) \left(\frac{q_1}{q_2} \right)^2 \times \left[\frac{q_1}{q_2} I^\pm(\omega_2) + \left(1 - \frac{q_1}{q_2} \right) I_S(\omega_2) \right], \quad (13a)$$

$$I^\pm(\omega_1) \leq \left(\frac{q_1}{q_2} \right)^2 \left[\frac{q_1}{q_2} I^\pm(\omega_2) + \left(1 - \frac{q_1}{q_2} \right) I_S(\omega_2) \right]. \quad (13b)$$

Equation (7) implies that

$$\frac{I_S(\omega_2)}{q_2^2} - \frac{I_S(\omega_1)}{q_1^2} \geq 0 \quad (8a)$$

and

$$\frac{I_S(\omega_2)}{q_2^2} - \frac{I_S(\omega_1)}{q_1^2} \leq \left(\frac{q_2^2 - q_1^2}{N^2 - q_1^2} \right) \frac{I_S(\omega_2)}{q_2^2}. \quad (8b)$$

Hence it follows from (8a) and (8b) that

$$\left(1 - \frac{q_2^2 - q_1^2}{N^2 - q_1^2} \right) \left(\frac{q_1}{q_2} \right)^2 I_S(\omega_2) \leq I_S(\omega_1) \leq \left(\frac{q_1}{q_2} \right)^2 I_S(\omega_2). \quad (9)$$

2. Bounds on $I^\pm(\omega)$

Similarly, one gets the lower and upper bounds for the high-energy dispersion integral $I^\pm(\omega)$ by noting that $I^\pm(\omega)/q$ is an increasing function of q since $\sigma_S \pm (\omega/\omega') \sigma_A$ is always positive in the range of integration ($\omega < \omega'$). For ω in the high-energy region ($\omega \gg \mu$), one can set $\omega = q$. Now consider the expression

From here onward let us define

$$\begin{aligned} \epsilon(\omega_1, \omega_2) &= \frac{q_2^2 - q_1^2}{N^2 - q_1^2} \\ &= \frac{\omega_2^2 - \omega_1^2}{N^2 - q_1^2}. \end{aligned}$$

Inequalities (13a) and (13b) are valid for both the $\pi^+ p$ and $\pi^- p$ high-energy dispersion integrals. By

applying (13a) and (13b) to the symmetric high-energy dispersion integral

$$I_S(\omega_1) = \frac{1}{2} [I^+(\omega_1) + I^-(\omega_2)]$$

we get back inequality (9).

3. Bounds on $I_A(\omega)$

Strict inequalities similar to Eqs. (9) and (13) cannot be derived for the high-energy dispersion integral $I_A(\omega)$ since there is no positivity condition for $\sigma_A(\omega')$. However, $I_A(\omega)$ can be bounded in terms of measurable quantities as follows:

$$|I_A(\omega)| \leq \frac{q^2}{2\pi^2} \left| \int_N^\infty \left(\frac{\mu}{\omega'} \right) \frac{\sigma_S(\omega')}{\omega'^2 - \omega^2} d\omega' \right| \leq \frac{\mu}{N} I_S(\omega), \quad (14)$$

where we have used the obvious fact that $|\sigma_A(\omega)| \leq \sigma_S(\omega)$.

Between two points $\omega_2 > \omega_1$ one can also have the following inequality:

$$\left| \frac{I_A(\omega_1)}{q_1^2} - \frac{I_A(\omega_2)}{q_2^2} \right| < \left(\frac{\mu}{N} \right) \epsilon(\omega_2, \omega_1) \frac{I_S(\omega_2)}{q_2^2}, \quad (15)$$

from which we deduce that

$$I_A(\omega_1) > \left(\frac{q_1}{q_2} \right)^2 \left[I_A(\omega_2) - \left(\frac{\mu}{N} \right) \epsilon(\omega_2, \omega_1) I_S(\omega_2) \right], \quad (16a)$$

$$I_A(\omega_1) < \left(\frac{q_1}{q_2} \right)^2 \left[I_A(\omega_2) + \left(\frac{\mu}{N} \right) \epsilon(\omega_2, \omega_1) I_S(\omega_2) \right]. \quad (16b)$$

As will be shown below, inequalities (14)–(16) can give a useful limit on $I_A(\omega)$ in certain cases, especially when $\mu/N \ll 1$ and ω is not too large. This is particularly important since there is no alternative way of learning about $I_A(\omega)$ except by measuring the total cross sections up to infinity, which cannot be done.

C. Application

1. Test of Energy Variation of $I_S(\omega)$ and $I^\pm(\omega)$ as Predicted by Dispersion Relation

The usefulness of inequalities (9) and (13) lies in the fact that for $\omega_1, \omega_2 \ll N$, $\epsilon(\omega_1, \omega_2)$ becomes very small compared to unity, so that the differences between the lower and upper bounds for $I_S(\omega_1)$ and $I^\pm(\omega_1)$ are small. More explicitly, this difference [$\Delta I_S(\omega_1)$ or $\Delta I^\pm(\omega_1)$] satisfies

$$\frac{\Delta I_S(\omega_1)}{I_S(\omega_1)} \leq \frac{\epsilon(\omega_1, \omega_2)}{1 - \epsilon(\omega_1, \omega_2)} \quad (17a)$$

and

$$\frac{\Delta I^\pm(\omega_1)}{I^\pm(\omega_1)} \leq \frac{\epsilon(\omega_1, \omega_2)}{1 - \epsilon(\omega_1, \omega_2)}, \quad (17b)$$

where $\epsilon(\omega_1, \omega_2) = (\omega_2^2 - \omega_1^2)/(N^2 - q_1^2)$ is a monotonically decreasing function of ω_1 (ω_2 held fixed) and has a maximum when ω_1 is smallest. To have an idea of the order of magnitude of $\Delta I_S(\omega)/I_S(\omega)$ [or $\Delta I^\pm(\omega)/I^\pm(\omega)$], let us take $N = 60$ GeV and choose ω, ω_2 in the region 8–20 GeV. At 8 GeV, $\epsilon(\omega, \omega_2) = 9\%$; hence in this region $\epsilon(\omega, \omega_2) \leq 9\%$.

Thus in all practical applications, for ω lying in a narrow interval, inequalities (9) and (13) enable us to determine $I_S(\omega)$ or $I^\pm(\omega)$ in terms of its value at another suitably chosen ω_2 , depending on the accuracy required and on experimental considerations. Thus, if the dispersion relation is valid, the high-energy integral $I_S(\omega)$ should lie in a narrow region defined by the straight line $I_S(\omega_2)(q/q_2)^2$ and the curve $I_S(\omega_2)[1 - \epsilon(\omega, \omega_2)(q/q_2)^2]$ plotted against $(q/q_2)^2$, with $\omega < \omega_2$ and ω_2 held fixed. We have

$$[1 - \epsilon(\omega, \omega_2)] \left(\frac{q}{q_2} \right)^2 \leq I_S(\omega) \leq \left(\frac{q}{q_2} \right)^2 I_S(\omega_2). \quad (18)$$

Similarly, for $I^\pm(\omega)$,

$$[1 - \epsilon(\omega, \omega_2)] \left(\frac{q}{q_2} \right)^2 \left[\frac{q}{q_2} I^\pm(\omega_2) + \left(1 - \frac{q}{q_2} \right) I_S(\omega_2) \right] \leq I^\pm(\omega) \leq \left(\frac{q}{q_2} \right)^2 \left[\frac{q}{q_2} I^\pm(\omega_2) + \left(1 - \frac{q}{q_2} \right) I_S(\omega_2) \right]. \quad (19)$$

One can now test the dispersion relation either by comparing the experimental values of $I_S(\omega)$ and $I^\pm(\omega)$ with the limiting values determined by inequalities (18) and (19) or by comparing the measured values of $\text{Re} f_S(\omega)$ and $\text{Re} f^\pm(\omega)$ with the lower and upper bounds given by

$$\text{Re} f_S(\omega) \geq f_S(\mu) + \frac{f^2}{M} + J_S(\omega) + [1 - \epsilon(\omega, \omega_2)] \left(\frac{q}{q_2} \right)^2 I_S(\omega_2), \quad (20a)$$

$$\text{Re} f_S(\omega) \leq f_S(\mu) + \frac{f^2}{M} + J_S(\omega) + \left(\frac{q}{q_2} \right)^2 I_S(\omega_2). \quad (20b)$$

Similarly for $\text{Re} f^\pm(\omega)$ one gets

$$\text{Re} f^\pm(\omega) \geq f_S(\mu) \pm \frac{\omega}{\mu} f_A(\mu) \pm \frac{\omega}{\mu} \frac{2f^2}{\mu} \left(1 - \frac{\mu^2}{4M^2} \right)^{-1} + J^\pm(\omega) + [1 - \epsilon(\omega, \omega_2)] \left(\frac{q}{q_2} \right)^2 \left[\left(\frac{q}{q_2} \right) I^\pm(\omega_2) + \left(1 - \frac{q}{q_2} \right) I_S(\omega_2) \right], \quad (21a)$$

$$\text{Re} f^\pm(\omega) \leq f_S(\mu) \pm \frac{\omega}{\mu} f_A(\mu) \pm \frac{\omega}{\mu} \frac{2f^2}{\mu} \left(1 - \frac{\mu^2}{4M^2} \right)^{-1} + J^\pm(\omega) + \left(\frac{q}{q_2} \right)^2 \left[\left(\frac{q}{q_2} \right) I^\pm(\omega_2) + \left(1 - \frac{q}{q_2} \right) I_S(\omega_2) \right]. \quad (21b)$$

Since $\epsilon(\omega_1, \omega_2) = (\omega_2^2 - \omega_1^2)/(N^2 - \omega_1^2)$ is a decreasing function of the cutoff energy N when ω_1, ω_2 are held fixed, the more we increase the cutoff energy by measuring the total cross sections at higher energies, the closer are the lower and upper bounds for $\text{Re}f_S(\omega)$. For example, with $N=300$ GeV (the NAL energy), ω in the range 10–20 GeV, $\omega_2=20$ GeV, one gets

$$\epsilon(\omega, \omega_2) \leq 0.3 \times 10^{-2},$$

which shows that the lower and upper bounds on $I_S(\omega)$ and $I^\pm(\omega)$ differ at most by 0.3%.

At present the data on $\text{Re}f^\pm(\omega)$ are available² at energies ω in the range 8–20 GeV and the total cross sections $\sigma^\pm(\omega')$ are measured⁴ up to $N=60$ GeV. The factor $\epsilon(\omega, \omega_2)$ at worst is less than 9%, which is smaller than the errors of the experimental values of $\text{Re}f^\pm(\omega)$. With these data we have compared the experimental values of

$$\alpha_S(\omega) = \frac{\text{Re}f_S(\omega)}{\text{Im}f_S(\omega)}$$

and

$$I_S(\omega)$$

with those predicted by inequalities (18) and (20) in terms of the cutoff dispersion integral $J_S(\omega)$ and the value of $\text{Re}f_S(\omega)$ at $\omega=20$ GeV. The re-

sults of the calculation show that $\alpha_S(\omega)$ lie well inside the two limiting curves representing the lower and upper bounds of $\alpha_S(\omega)$ (Fig. 1) and that $I_S(\omega)$ approximately lie on the straight line $(q/q_2)^2 I_S(\omega_2)$ (Fig. 2). These results can be considered a consistent test of the validity of the dispersion relation and that to an accuracy of better than 9% one can write approximately

$$\text{Re}f_S(\omega) = \frac{f^2}{M} + f_S(\mu) + J_S(\omega) + q^2 \left[\frac{I_S(\omega_2)}{q_2^2} \right], \quad (22)$$

where

$$\frac{I_S(\omega_2)}{q_2^2} = \frac{1}{2\pi^2} \int_N^\infty \frac{\sigma_S(\omega') d\omega'}{\omega'^2 - \omega_2^2}. \quad (23)$$

The values 0.08 for f^2 and -0.002 ± 0.004 for $f_S(\mu)$ have been used. The results are insensitive to the uncertainties in the determination of f^2 and $f_S(\mu)$ [these quantities give a negligible contribution to the bounds of $\text{Re}f_S(\omega)$] and to the low-energy total cross section measurement.

In terms of the experimental quantities at 20 GeV, the lower and upper bound of $\text{Re}f_S(\omega)$ for $\omega > 20$ GeV can also be predicted from (18); in this case, due to the factor $(\omega^2 - \omega_2^2)/(N^2 - \omega_2^2)$, the difference between the bounds is as large as 20% at $\omega=30$ GeV, reaching 60% at 40 GeV, making the bounds useless in determining $\text{Re}f_S(\omega)$; further-

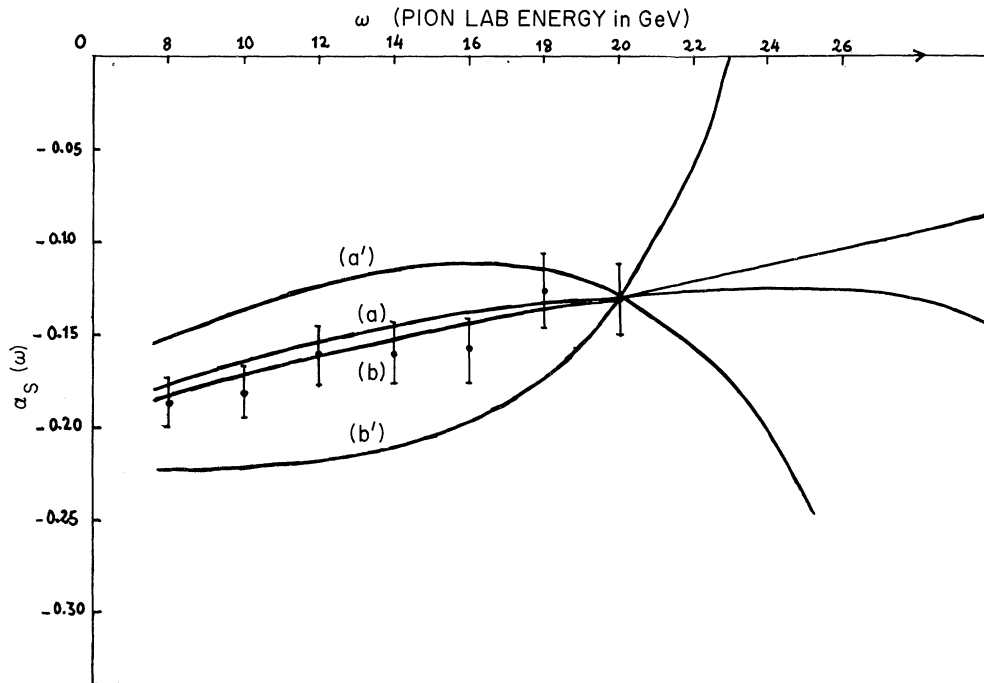


FIG. 1. Experimental data (\bullet) on $\alpha_S(\omega) = \text{Re}f_S(\omega)/\text{Im}f_S(\omega)$ and the theoretical lower and upper bounds of $\alpha_S(\omega)$ normalized at $\omega=20$ GeV. The curves (a) and (b) are theoretical upper and lower limits for $N=60$ GeV; the curves (a') and (b') are the theoretical upper and lower limits for $N=30$ GeV.

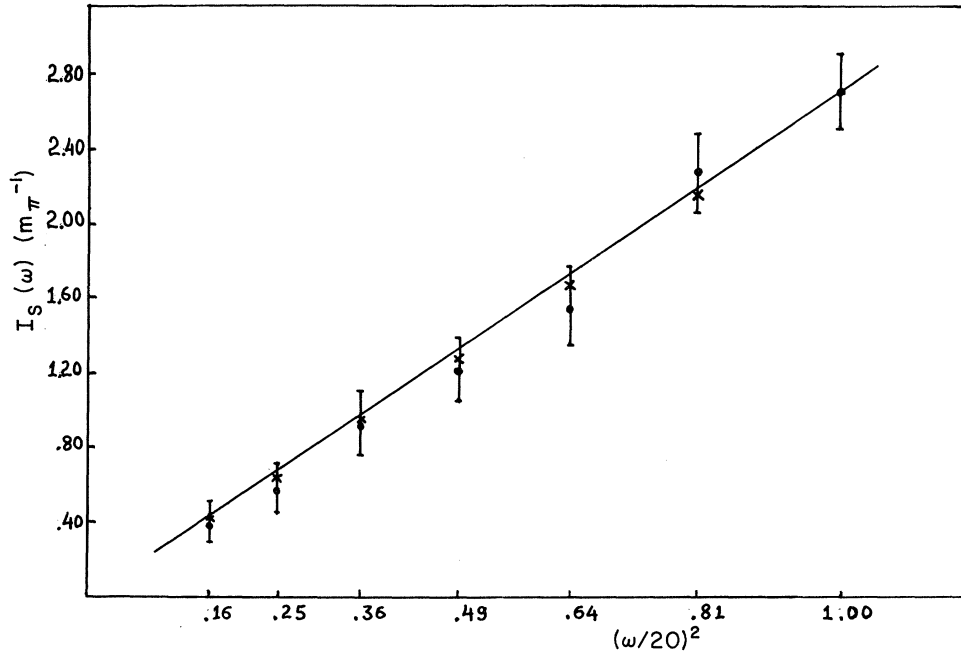


FIG. 2. Experimental values (\ast) of the high-energy dispersion integral $I_S(\omega)$ and the theoretical lower (\times) and upper (solid curve) bounds for $I_S(\omega)$ normalized at 20 GeV, $N=60$ GeV.

more, for $\omega > \omega_2$, because of the factor $(q/q_2)^2$, the errors of $\text{Re}f_S(\omega_2)$ cause the errors of these bounds increasingly large with increasing ω .

As we lower the cutoff energy N , the differences between the lower and upper bounds for $\text{Re}f_S(\omega)$ and $I_S(\omega)$ become larger so that Eqs. (18) and (20) become less effective in the analysis of the dispersion relation for $\text{Re}f_S(\omega)$. As an example, we give in Figs. 1 and 3 the results of calculation for $N=30$ GeV, pretending that there were no data on cross sections beyond 30 GeV. The results show that the lower and upper limits of $\alpha_S(\omega)$ and $I_S(\omega)$ become rather loose and the experimental points clearly lie within the two limiting curves (Figs. 1 and 3).

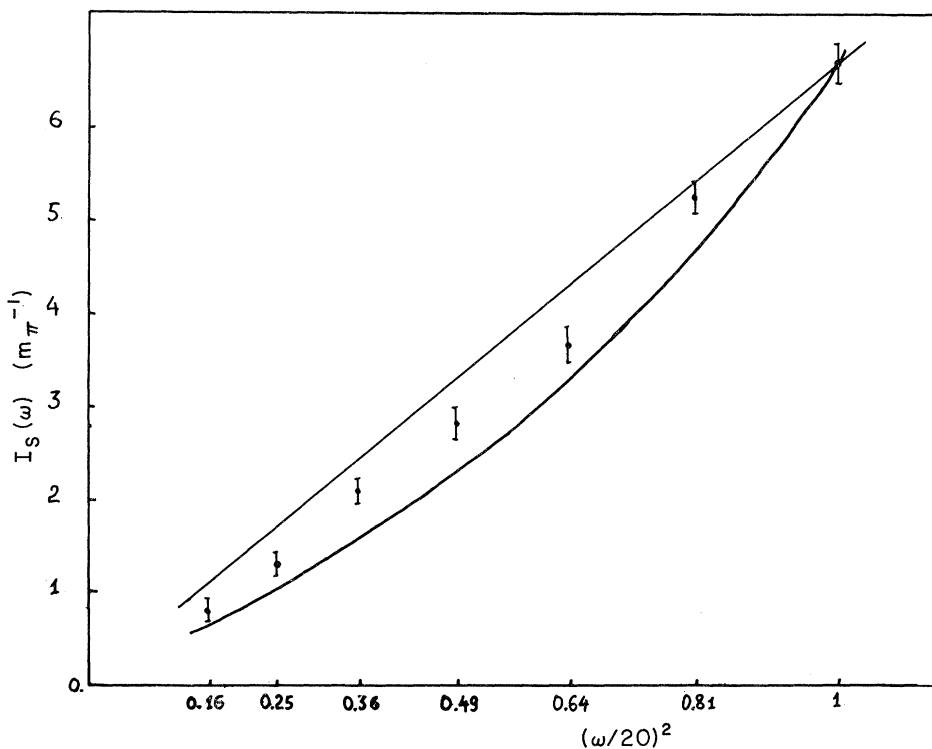
Thus, in order to test the dispersion relation it is necessary to have the total cross sections measured at energies much higher than the energies at which $\text{Re}f^\pm(\omega)$ are measured.

2. Remarks on the Test of Dispersion Relation for $f_A(\omega)$ and $f^\pm(\omega)$

It is apparent from the once-subtracted dispersion relation for $f_A(\omega)$ [Eq. (5)] that one cannot test the dispersion relation for $f_A(\omega)$ at high energy in the same way as for $f_S(\omega)$ since there is no positivity condition for $\sigma_A(\omega')$ which enables us to study the energy variation of $I_A(\omega)$; furthermore, in contrast with the case of the unsubtracted dis-

persion relation, since the contributions to $\text{Re}f_A(\omega)$ from the subtraction constants [f^2 and $f_A(\mu)$] are very large compared with $(\mu/\omega)\text{Re}f_A(\omega)$ at high energy (8–20 GeV), an accurate knowledge of f^2 and $f_A(\mu)$ is required in the analysis of the dispersion relation. An alternative way is to look at cases in which $I_A(\omega)$ is small compared with $(\mu/\omega)\text{Re}f_A(\omega)$ and to study the energy variation of $(\mu/\omega)\text{Re}f_A(\omega)$. As will be shown below (Sec. III), the present Serpukhov data up to 60 GeV give the upper bound of $|I_A(\omega)|$ a value $(1.0 \pm 0.2) \times 10^{-3} (1/\mu)$ which is 30% relative to $(\mu/\omega)\text{Re}f_A(\omega)$ at 8 GeV and larger at other energies in the 8–20-GeV region. This shows that one cannot neglect $I_A(\omega)$ in the analysis of dispersion relation for $f_A(\omega)$ with present data on total cross sections. However, if the data on the total cross sections are available up to 300 GeV, then $|I_A(\omega)|$ will be much reduced [less than 0.2% relative to $(\mu/\omega)\text{Re}f_A(\omega)$], so that one can neglect $I_A(\omega)$ and test the energy variation of $(\mu/\omega)\text{Re}f_A(\omega)$ without requiring an accurate knowledge of f^2 and $f_A(\mu)$. This will be clear later when we come to Eq. (39) of Sec. III.

As for the $f^\pm(\omega)$ amplitude, provided that $[2f^2/\mu + f_A(\mu)]$ is determined with high precision by some independent methods, an analysis similar to the one for $f_S(\omega)$ can be carried out in a straightforward way with the help of (19) and (21). This is not possible with the present determinations of f^2 and $f_A(\mu)$. [The experimental errors

FIG. 3. The same as Fig. 2 with $N = 30$ GeV.

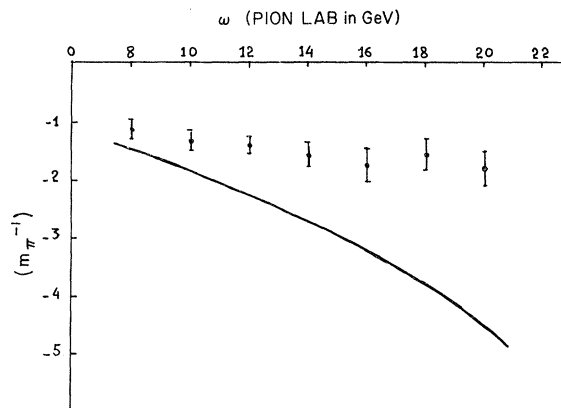
of f^2 and $f_A(\mu)$ are appreciable and, due to the presence of the factor $\omega/\mu \gg 1$, are comparable to the errors of $\text{Re}f^\pm(\omega)$.] For this reason we shall not make an analysis for $f^\pm(\omega)$. As with the case of $f_A(\omega)$ discussed above, to test the energy variation for $f^\pm(\omega)$ one must reduce the high-energy contribution $(\omega/\mu)I_A(\omega)$ relative to $\text{Re}f^\pm(\omega)$ by measuring the total cross sections up to energy much higher than that at present; in fact the data at Serpukhov give $(\omega/\mu)|I_A(\omega)|/\text{Re}f^\pm(\omega) \approx 10\text{--}30\%$ for ω in the 8–20-GeV region; this relative contribution will be reduced by a factor of 25 with NAL data. Thus one can test the dispersion relation to a reasonable accuracy by ignoring $I_A(\omega)$.

3. Upper Bound on the Total Cross Sections at Energies Above the Cutoff Energy

The method of analysis discussed above does not provide a stringent test of the dispersion relation since it does not impose any condition on the total cross sections beyond the cutoff energy. In fact without a measurement of the total cross sections beyond the cutoff energy, all one can tell from the dispersion relation is that

$$\text{Re}f_S(\omega) > \frac{f^2}{M} + f_S(\mu) + J_S(\omega). \quad (24)$$

The data on $\text{Re}f_S(\omega)$ in the range 8–20 GeV show that (24) is easily satisfied and that as ω varies from 8 to 20 GeV the discrepancy between the experimental values and the right-hand side of (24) becomes larger, as can be seen in Fig. 4. This discrepancy represents the value of $I_S(\omega)$, which increases approximately quadratically with ω . Thus the lack of knowledge of $I_S(\omega)$ makes it impossible to have a sensitive test of dispersion relation in the 8–20-GeV region with present data

FIG. 4. Contribution to $\text{Re}f_S(\omega)$ (\cdot) from the cutoff dispersion integral $J_S(\omega)$ (solid curve).

on total cross sections up to 60 GeV.

A sensitive test can only be done with more data on total cross sections so as to reduce the contribution of $I_S(\omega)$ to $\text{Re}f_S(\omega)$. To have an idea of the magnitude of $I_S(\omega)$, let us take $\omega = 20$ GeV; at this energy $I_S(\omega) \approx 2|\text{Re}f_S(\omega)|$ for $N = 60$ GeV; assuming that $\sigma(\omega')$ is constant from 60 to 300 GeV, a simple calculation shows that $I_S(\omega)$ is reduced by a factor of 5, i.e., $I_S(\omega) \approx 0.4|\text{Re}f_S(\omega)|$ at 20 GeV; below 20 GeV, $I_S(\omega)$ becomes very small compared with $\text{Re}f_S(\omega)$. Conversely, assuming the validity of the dispersion relation, one can learn about the total cross section in an energy interval above the cutoff energy by considering the quantity

$$\frac{I_S(\omega)}{\omega^2} = \frac{1}{2\pi^2} \int_N^\infty \frac{\sigma_S(\omega')}{\omega'^2 - \omega^2} d\omega'. \quad (25)$$

For any energy interval (M_1, M_2) (with $N \leq M_1 < M_2$), it is obvious that

$$\frac{I_S(\omega)}{\omega^2} \geq \frac{1}{2\pi^2} \int_{M_1}^{M_2} \frac{\sigma_S(\omega')}{\omega'^2 - \omega^2} d\omega'. \quad (26)$$

Thus experimental data on $I_S(\omega)$ give predictions on $\sigma_S(\omega')$ in (M_1, M_2) . This is a more stringent test of dispersion relation for M_2 high enough ($M_2 \geq 300$ GeV), since the right-hand side of (26) gives a dominant contribution to $\text{Re}f_S(\omega)$, as seen in the above example. A better way of handling (26) by using the averaged dispersion relation will be given in the next sections.

D. Average Dispersion Relation

As pointed out in the Introduction, in the analysis of dispersion relation one usually encounters the principal-part integration. In practice, in order to carry out the principal-part integration, it is necessary to assume a smoothness for the behavior of the total cross sections in the neighborhood of the singularity $\omega' = \omega$ of the integrand.

This can be avoided by considering the dispersion relation for the energy-weighted average amplitude $\langle f^\pm \rangle$, $\langle f_{S,A} \rangle$ over an energy interval (ω_1, ω_2) defined as

$$\langle f^\pm(\omega_1, \omega_2) \rangle = \frac{\int_{\omega_1}^{\omega_2} f^\pm(\omega) \rho(\omega) d\omega}{\int_{\omega_1}^{\omega_2} \rho(\omega) d\omega}, \quad (27a)$$

$$\langle f_{S,A}(\omega_1, \omega_2) \rangle = \frac{\int_{\omega_1}^{\omega_2} f_{S,A}(\omega) \rho(\omega) d\omega}{\int_{\omega_1}^{\omega_2} \rho(\omega) d\omega}. \quad (27b)$$

This procedure was first pointed out⁵ by Khuri and Kinoshita, and Martin, who set $\omega_1 = \mu$.

The reason for working with this weighted average amplitude is that in carrying out the calcula-

tion of $\langle \text{Re}f_{S,A}(\omega_1, \omega_2) \rangle$ or $\langle \text{Re}f^\pm(\omega_1, \omega_2) \rangle$ using the dispersion relation (2)–(5), one encounters only the logarithmic singularity in the expression for $\langle J_{S,A}(\omega_1, \omega_2) \rangle$; for example, with $\rho(\omega) = 1$, one gets ($\omega \approx q$)

$$\begin{aligned} \langle J_{S,A}(\omega_1, \omega_2) \rangle &= \frac{1}{2\pi^2} \int_0^N dq' \sigma_{S,A}(\omega') \\ &\times \left[\frac{q'}{2(q_2 - q_1)} \ln \left| \frac{q' + q_2}{q' - q_2} \frac{q' - q_1}{q' + q_1} \right| - 1 \right]. \quad (28) \end{aligned}$$

Consequently the resulting integral $\langle J_{S,A}(\omega_1, \omega_2) \rangle$ is less sensitive to the assumption of the smooth behavior of $\sigma^\pm(\omega')$ than the ordinary dispersion integral $J_{S,A}(\omega)$. A practical usefulness of this energy-weighted dispersion integral is that the error of $\langle J_{S,A}(\omega_1, \omega_2) \rangle$ due to the experimental errors of $\sigma^\pm(\omega')$ is much reduced.

We now apply the above energy-weighted dispersion relation to the experimental analysis of the dispersion relation.

1. Upper Bound on Total Cross Sections

The prediction for the bound on total cross sections given in the previous section can now be obtained in the following way: Consider the expression for $\langle \text{Re}f_S(\omega_1, \omega_2) \rangle$ with $\rho(\omega) = 1$ [for a reason which will become clear below we have chosen $\rho(\omega) = 1$] ($\omega_1 \approx q_1$, $\omega_2 \approx q_2$):

$$\begin{aligned} \langle \text{Re}f_S(\omega_1, \omega_2) \rangle &= f_S(\mu) + \frac{f^2}{M} \left(1 - \frac{\mu^2}{4M^2} \right)^{-1} \\ &+ \langle J_S(\omega_1, \omega_2) \rangle + \langle I_S(\omega_1, \omega_2) \rangle, \quad (29) \end{aligned}$$

where

$$\langle J_S(\omega_1, \omega_2) \rangle = \frac{1}{2\pi^2} \int_0^N dq' K(\omega'; \omega_1, \omega_2) \sigma_S(\omega'),$$

$$\langle I_S(\omega_1, \omega_2) \rangle = \frac{1}{2\pi^2} \int_N^\infty dq' K(\omega'; \omega_1, \omega_2) \sigma_S(\omega'),$$

and

$$K(\omega'; \omega_1, \omega_2) = \left[\frac{1}{q_2 - q_1} \left(\frac{q'}{2} \ln \left| \frac{q' + q_2}{q' - q_2} \frac{q' - q_1}{q' + q_1} \right| \right) - 1 \right].$$

For $N < M_1 < M_2$, because of the positivity of $\sigma_S(\omega')$, it is obvious that

$$\langle I_S(\omega_1, \omega_2) \rangle > \frac{1}{2\pi^2} \int_{M_1}^{M_2} dq' K(\omega'; \omega_1, \omega_2) \sigma_S(\omega'). \quad (30)$$

For the experimental evaluation of (30), we shall

choose $\omega_1 = 8$ GeV, $\omega_2 = 20$ GeV. In particular, to get a strict inequality we choose $M_1 = N$. From the experimental data on $\text{Re} f^{\pm}(\omega)$ in the 8–20-GeV region and the total cross sections up to 60 GeV, we deduce from (30) that

$$\int_N^{M_2} dq' K(\omega'; \omega_1, \omega_2) 2\sigma_s(\omega') \leq 154 \pm 8 \text{ mb GeV}. \quad (31)$$

A more transparent but somewhat less strict bound than (31) can be obtained by noting that in the range of integration the following inequality is valid:

$$K(\omega'; \omega_1, \omega_2) > \frac{1}{3}(\omega_1^2 + \omega_1\omega_2 + \omega_2^2) \frac{1}{\omega'^2}.$$

Hence we obtain the following inequality:

$$\int_N^{M_2} \frac{2\sigma_s(\omega')}{\omega'^2} d\omega' < 0.74 \pm 0.04 \text{ mb GeV}^{-1}. \quad (31')$$

If the experimental values for $\text{Re} f_s(\omega)$ were available for energy higher than 20 GeV, inequality (31') would become loose and lead to a poor bound for σ_s . In this case, we should use inequality (31).

In contrast with previous considerations,⁵ we want to amplify the high-energy contribution of $I_s(\omega)$ to improve the accuracy of (31). This is so because the experimental relative errors of $I_s(\omega)$ decrease with increasing ω . Hence the choice $\rho(\omega) = 1$ was made.

To have an idea of the magnitude of the total cross sections inferred from (31), let us suppose that between 60 and 500 GeV $\sigma_s(\omega')$ stays constant; then (31) implies that

$$2\sigma_s(\omega') \leq 50.1 \pm 3 \text{ mb},$$

to be compared with the value of 47.4 ± 0.4 mb at 60 GeV. This rules out any appreciable increase in $\sigma_s(\omega')$ between 60 and 500 GeV.

To test the usefulness of (30), let us pretend that there were no data on the total cross sections above 30 GeV. The right-hand side of (31) now with $N = 30$ GeV gives 359.7 ± 8 mb GeV, which is larger by approximately a factor of 2 than the right-hand side of (31). Because the Serpukhov data obey this new inequality, we can conclude that they are a test of the dispersion relation.

2. Test of Energy Variation of the Averaged Dispersion Relation

By straightforward integration of inequality (9) in the variables ω_1 and ω_2 over (a, b) and (c, d) , respectively, with $a, b < c, d$, one could also derive the strict bounds for $\langle I_s(a, b) \rangle$ in terms of $\langle I_s(c, d) \rangle$. The test of dispersion relation consists of comparing the limits for $\langle \text{Re} f_s(a, b) \rangle$ with the

experimental value. For example, for $\rho(\omega) = 1$, we have the inequality

$$\frac{1}{3} \left(\frac{a^2 + ab + b^2}{d^2} \right) \left(1 - \frac{d^2 - a^2}{N^2 - c^2} \right) \langle I_s(c, d) \rangle \leq I_s(a, b) \leq \frac{1}{3} \left(\frac{a^2 + ab + b^2}{c^2} \right) \langle I_s(c, d) \rangle, \quad (32)$$

and we have similar bounds for $\langle \text{Re} f_s(a, b) \rangle$ in terms of $\langle \text{Re} f_s(c, d) \rangle$ and $\langle J_s(a, b) \rangle$ and $\langle J_s(c, d) \rangle$ obtained from the above inequality.

As an example, we have applied the above method to the analysis of averaged dispersion for $(a, b) = (8, 16)$, $(c, d) = (18, 20)$. The results of the calculation show that the experimental data on $\langle \text{Re} f_s(a, b) \rangle$ are consistent with dispersion relation.

III. TEST OF DISPERSION RELATION AT LOW ENERGY OR THE DETERMINATION OF LOW-ENERGY πN PARAMETERS

A. Determination of the Pion-Nucleon Coupling Constant

1. Determination of f^2 with Present Data

It has been shown in the previous section [Eq. (14)] that the high-energy dispersion integral $I_A(\omega)$ can be bounded in terms of measurable quantities:

$$|I_A(\omega)| < \frac{\mu}{N} I_s(\omega).$$

One can now make use of the above upper limit on $|I_A(\omega)|$ to determine f^2 . We first note that $\text{Re} f_A(\omega)$ is experimentally small at high energy and furthermore its contribution is suppressed by a very important factor $\mu/\omega \approx 1.8 \times 10^{-2}$ ($\omega = 8$ GeV). Consequently, at high energy, Eq. (5) does not depend much on $\text{Re} f_A(\omega)$. Equation (5) reads

$$\left(1 - \frac{\mu^2}{4M^2} \right)^{-1} \frac{2f^2}{\mu} = \frac{\mu}{\omega} \text{Re} f_A(\omega) - f_A(\mu) - J_A(\omega) - I_A(\omega). \quad (33)$$

We shall now prove that $I_A(\omega)$ gives a negligible contribution to f^2 when $\omega \lesssim 10$ GeV. In terms of $\text{Re} f_s(\omega)$ and $J_s(\omega)$, $|I_A(\omega)|$ is given by

$$|I_A(\omega)| < \epsilon - \frac{\mu}{N} \left(1 - \frac{\mu^2}{4M^2} \right)^{-1} \frac{f^2}{M} - \frac{\mu}{N} f_s(\mu), \quad (34)$$

with

$$\epsilon \equiv \frac{\mu}{N} [\text{Re} f_s(\omega) - J_s(\omega)]. \quad (35)$$

To see that the bound of $|I_A(\omega)|$ does not effectively depend on f^2 and $f_s(\mu)$, we note that the pion-

nucleon coupling constant f^2 on the right-hand side of (34) is multiplied by μ/NM , whereas it is multiplied by $2/\mu$ on the right-hand side of (33). Thus to an accuracy of $\mu^2/2MN \approx 1.7 \times 10^{-4}$ (M = nucleon mass) we can neglect it on the right-hand side of (34); similarly the neglecting of $\text{Re} f_s(\mu)$ on the right-hand side of (34) represents a loss of an accuracy of

$$\frac{\mu}{N} \frac{f_s(\mu)}{f_A(\mu)} \approx 2.5 \times 10^{-4},$$

using

$$\frac{f_s(\mu)}{f_A(\mu)} = \frac{1}{10}.$$

Allowing a very considerable uncertainty in the determination of this last ratio, we can safely conclude that to an accuracy better than 1 part in 1000, f^2 is given by

$$\left(1 - \frac{\mu^2}{4M^2}\right)^{+1} [X(\omega) - \epsilon] \leq \frac{2f^2}{\mu} \leq \left(1 - \frac{\mu^2}{4M^2}\right)^{-1} [X(\omega) + \epsilon], \quad (36)$$

where

$$X(\omega) = \left[\frac{\mu}{\omega} \text{Re} f_A(\omega) - f_A(\mu) - J_A(\omega) \right].$$

Thus the bound on $|I_A(\omega)|$ is just ϵ . In order to make inequalities (36) as strict as possible, we must minimize ϵ . With the available data on $\text{Re} f^\pm(\omega)$ from 8 to 20 GeV and the total cross sections measured up to 60 GeV, since $I_s(\omega)$ is an increasing function of ω , ϵ is smallest at 8 GeV. Hence we set $\omega = 8$ GeV; at this energy, the measurement of Foley *et al.*² gives $\text{Re} f_s(\omega) = (-1.16 \pm 0.12)\mu^{-1}$ and the value of the dispersion integral $J_s(\omega)$ is numerically computed to be $(-1.54 \pm 0.01)\mu^{-1}$, which leads to

$$\epsilon = (0.9 \pm 0.3) \times 10^{-3} \mu^{-1} \quad (\text{in units of } \mu^{-1} = 1.41 \text{ fm}).$$

Alternatively we note that it is possible to get the bound for $|I_A(\omega)|$ without involving $f_s(\mu)$ and f^2 by making use of the experimental data on $\text{Re} f_s(\omega)$ at two points ω and $\bar{\omega}$ far away from each other ($\bar{\omega} > \omega$), since $f_s(\mu)$ and f^2 disappear in the expression for the difference $\text{Re} f_s(\bar{\omega}) - \text{Re} f_s(\omega)$. Equation (36) then becomes rigorously valid except that ϵ is now given by

$$\epsilon = \left(\frac{\mu}{N}\right) \left(\frac{q^2}{\bar{q}^2 - q^2}\right) [\text{Re} f_s(\bar{\omega}) - \text{Re} f_s(\omega) + J_s(\omega) - J_s(\bar{\omega})], \quad (37)$$

For $\omega = 8$ GeV, $\bar{\omega} = 18$ GeV, using $\text{Re} f_s(18) = (-1.57 \pm 0.18)\mu^{-1}$ and $J_s(18) = (-3.77 \pm 0.02)\mu^{-1}$,

one gets

$$\epsilon = (1.00 \pm 0.2) \times 10^{-3} \mu^{-1},$$

which agrees with the value found above. Since the experimental value of $2\epsilon/X(\omega)$ is 2%, it is clear from (36) that the upper bound for f^2 differs from its lower bound by about 1%. Within this accuracy, we have the sum rule

$$\frac{2f^2}{\mu} = \left(1 + \frac{\mu}{N}\right) (a_- - a_+) + \frac{\mu}{\omega} \text{Re} f_A(\omega) - \frac{q^2}{4\pi^2} \int_0^N \left(\frac{\mu}{\omega'}\right) \frac{dq' (\sigma^+ - \sigma^-)}{\omega'^2 - \omega^2}, \quad (38)$$

which is valid for $\omega \leq 8$ GeV and $\omega \gg \mu$. By the method of partial fractions, (38) can be written in terms of a cutoff integral and a small correction term in the square bracket:

$$\frac{2f^2}{\mu} = \left(1 + \frac{\mu}{M}\right) (a_- - a_+) + \frac{\mu}{4\pi^2} \int_0^N \frac{dq'}{\omega'} (\sigma^+ - \sigma^-) - \left[\frac{\mu}{4\pi^2} \text{P} \int_0^N \frac{q' d\omega'}{\omega'^2 - \omega^2} (\sigma^+ - \sigma^-) - \frac{\mu}{\omega} \text{Re} f_A(\omega) \right], \quad (39)$$

to be compared with the Goldberger-Miyazawa-Oehme sum rules⁶

$$\frac{2f^2}{\mu} \left(1 - \frac{\mu^2}{4M^2}\right)^{-1} = \left(1 + \frac{\mu}{M}\right) (a_- - a_+) + \frac{\mu}{4\pi^2} \int_\mu^\infty \frac{d\omega'}{q'} (\sigma^+ - \sigma^-) \quad (40)$$

derived long ago from an unsubtracted dispersion relation for $f_A(\omega)$.

To the extent that one can neglect $I_A(\omega)$, Eq. (39) shows that the correction term (the square bracket) is constant over the energy range where $I_A(\omega)$ is small compared with $(\mu/\omega) \text{Re} f_A(\omega)$. When this is the case, one can test the energy variation of the dispersion relation for $f_A(\omega)$ without requiring an accurate knowledge of the pion-nucleon coupling constant and the s -wave πN scattering lengths. As discussed in Sec. II, this happens when $N = 300$ GeV. At this cutoff energy, $I_A(\omega)$ becomes very small compared with $(\mu/\omega) \text{Re} f_A(\omega)$.

The integral on the right-hand side of (38) can be calculated numerically using the available data on $\sigma^\pm(\omega')$. We find that at $\omega = 8$ GeV

$$J_A(\omega) = (-0.0548 \pm 0.002) \mu^{-1}.$$

The data on $\text{Re} f^\pm(\omega)$ of Foley *et al.* give

$$\frac{\mu}{\omega} \text{Re} f_A(\omega) = (-0.003 \pm 0.0015) \mu^{-1} \text{ at } \omega = 8 \text{ GeV}.$$

Putting these values into (38) we arrive at

$$\frac{2f^2}{\mu} = \left(1 + \frac{\mu}{M}\right)(a_- - a_+) + (0.0518 \pm 0.0015)\mu^{-1}, \quad (41)$$

which is a relation involving the pion-nucleon coupling constant and $a_- - a_+$. A similar relation has been obtained by Höhler and Strauss.⁷ Using the charge-exchange data and assuming an asymptotic Regge behavior for the total cross sections, they showed that f^2 can be determined accurately in terms of $(a_- - a_+)$. Our result indicates that it is not necessary to make such an assumption. Equation (41) should be used with other relations derived in the next section to determine f^2 and a_{\pm} in terms of low-energy data. At present, the value

$$a_- - a_+ = (0.090 \pm 0.0023)\mu^{-1}$$

given by Hamilton⁸ yields

$$f^2 = 0.077 \pm 0.003,$$

which agrees more or less with the previously determined value.^{9,10} Of the total error (4%) in the determined value of f^2 , 1.5% comes from the determination of the scattering lengths, 1.2% from the measurement of $\text{Re}f_A(\omega)$ at 8 GeV, and 1.2% from the total cross section measurement. Undoubtedly these figures will be much reduced once new measurements of πN parameters become available at the new pion factories.

To reduce the errors of the dispersion integral due to the principal-part integration, and to improve the statistics, one should use all the available data on $\text{Re}f_A(\omega)$ in the region 8–20 GeV. This again can be done by using the energy-weighted average amplitude $\langle \text{Re}f_A(\omega_1, \omega_2) \rangle$ with an appropriate energy weight function $\rho(\omega)$. Since the upper bound on $|I_A(\omega)|$ increases quadratically with q^2 , [for example, this bound increases from $(1.0 \pm 0.2) \times 10^{-3} \mu^{-1}$ at $\omega = 8$ GeV to $4 \times (1.0 \pm 0.2) \times 10^{-3} \mu^{-1}$ at 16 GeV] and the difference in the lower and upper bounds for f^2 becomes larger, rendering Eq. (36) less effective in the determination of f^2 , we must choose $\rho(\omega)$ so as to have the contribution to $\langle \text{Re}f_A(\omega_1, \omega_2) \rangle$ mainly coming from $\text{Re}f_A(\omega)$ at the lower end of the energy interval.

A convenient choice for $\rho(\omega)$ is $1/\omega^2$. Equation (36) is now replaced by

$$\left(1 - \frac{\mu^2}{4M^2}\right) [\langle X(\omega_1, \omega_2) \rangle - \langle \epsilon \rangle] \leq \frac{2f^2}{\mu} \leq \left(1 - \frac{\mu^2}{4M^2}\right) [\langle X(\omega_1, \omega_2) \rangle + \langle \epsilon \rangle], \quad (36')$$

where

$$\langle X(\omega_1, \omega_2) \rangle = \frac{\int_{\omega_1}^{\omega_2} \frac{d\omega}{\omega^2} \left[\frac{\mu}{\omega} \text{Re}f_A(\omega) - f_A(\mu) - J_A(\omega) \right]}{\int_{\omega_1}^{\omega_2} \frac{d\omega}{\omega^2}}$$

and

$$\langle \epsilon \rangle = \frac{\int_{\omega_1}^{\omega_2} \frac{d\omega}{\omega^2} \text{Re}f_S(\omega) - J_S(\omega)}{\int_{\omega_1}^{\omega_2} \frac{d\omega}{\omega^2}} \approx \frac{\omega_1 \omega_2}{\omega_1^2} \epsilon.$$

In this way one gets better statistics at the expense of losing some accuracy in the determination of f^2 ; for example, for $\omega_1 = 8$, $\omega_2 = 20$, $\langle \epsilon \rangle \approx 2.5\epsilon = 2.5 \times (1.0 \pm 0.2) \times 10^{-3} \mu^{-1}$ and the lower and upper bounds of f^2 differ by 2.5%.

We have made a calculation for $\langle X(\omega_1, \omega_2) \rangle$; the result is that to an accuracy of better than 2.5% (actually better than this figure since here we used a very loose bound for $|I_A(\omega)|$) we get

$$f^2 = 0.077 \pm 0.002.$$

2. Improved Determination of f^2 with Future Experimental Data

Possible reductions of the high-energy dispersion integral $I_A(\omega)$ to increase the precision can be obtained as follows:

(a) *Using available experimental data on $\text{Re}f_A(\omega)$ at more than one energy in the region 8–20 GeV.* By this method one can determine quite accurately $I_A(\omega)$ in terms of other measurable quantities in a similar way as for $I_S(\omega)$. From Eqs. (16a) and (16b), one derives for ω_1, ω_2 far away from each other

$$\left(1 - \frac{\mu^2}{4M^2}\right) [X(\omega_1) + \Delta(\omega_1, \omega_2) + \delta(\omega_1, \omega_2)] \leq \frac{2f^2}{\mu} \leq \left(1 - \frac{\mu^2}{4M^2}\right) [X(\omega_1) + \Delta(\omega_1, \omega_2) - \delta(\omega_1, \omega_2)], \quad (42)$$

where

$$\Delta(\omega_1, \omega_2) = \frac{q_1^2}{q_2^2 - q_1^2} \left[\frac{\mu}{\omega_1} \text{Re}f_A(\omega_1) - J_A(\omega_1) + J_A(\omega_2) - \frac{\mu}{\omega_2} \text{Re}f_A(\omega_2) \right], \quad (43)$$

$$\delta(\omega_1, \omega_2) = \frac{\mu}{N} \frac{q_1^2}{N^2 - q_1^2} I_S(\omega_2). \quad (44)$$

It is clear from the definition [Eq. (44)] that $\delta(\omega_1, \omega_2)$ is smallest when both ω_1 and ω_2 are the lowest en-

ergies at which $\text{Re}f_A(\omega)$ are measured. Since ω_1 and ω_2 must be sufficiently far away from each other, to have an idea of the magnitude of $\delta(\omega_1, \omega_2)$, let us choose $\omega_1 = 8$ GeV, $\omega_2 = 16$ GeV; $\delta(\omega_1, \omega_2)$ is then equal to $(0.6 \pm 0.1) \times 10^{-4}$ ($N = 60$ GeV), which is only 0.04% relative to f^2 . More explicitly the discrepancy between the lower and upper bounds of f^2 in (42) [$2\delta(\omega_1, \omega_2)$] is only 0.08% relative to f^2 . Therefore to an accuracy of better than one part in a thousand, one can neglect this discrepancy and write

$$\frac{2f^2}{\mu} = \left(1 - \frac{\mu^2}{4M^2}\right) \left\{ -f_A(\mu) + \frac{\mu}{\omega_1} \text{Re}f_A(\omega_1) - J_A(\omega_1) + \left(\frac{q_1^2}{q_2^2 - q_1^2}\right) \left[\frac{\mu}{\omega_1} \text{Re}f_A(\omega_1) - \frac{\mu}{\omega_2} \text{Re}f_A(\omega_2) + J_A(\omega_2) - J_A(\omega_1) \right] \right\}. \quad (39')$$

It is easy to see that Eq. (39') in principle should give a better determination of f^2 than Eq. (39) since the high-energy dispersion integral $I_A(\omega)$ has been taken into account considerably by a small correction term

$$\Delta(\omega_1, \omega_2) = \frac{q_1^2}{q_2^2 - q_1^2} \left[\frac{\mu}{\omega_1} \text{Re}f_A(\omega_1) - \frac{\mu}{\omega_2} \text{Re}f_A(\omega_2) + J_A(\omega_2) - J_A(\omega_1) \right]$$

which can be written in the following form:

$$\left(\frac{q_1^2}{q_2^2 - q_1^2}\right) \left\{ \left[\frac{\mu}{\omega_1} \text{Re}f_A(\omega_1) - \frac{\mu}{4\pi^2} \text{P} \int_{\mu}^N \frac{q'd\omega'}{\omega'^2 - \omega_1^2} (\sigma^+ - \sigma^-) \right] - \left[\frac{\mu}{\omega_2} \text{Re}f_A(\omega_2) - \frac{\mu}{4\pi^2} \text{P} \int_{\mu}^N \frac{q'd\omega'}{\omega'^2 - \omega_2^2} (\sigma^+ - \sigma^-) \right] \right\}. \quad (45)$$

However, this apparent improved accuracy of f^2 due to a better bound of $I_A(\omega)$ is not easily realized in practice since the evaluation of $\Delta(\omega_1, \omega_2)$ introduces more experimental errors of $\text{Re}f_A(\omega)$ and $I_A(\omega)$ into the determination of f^2 [although these errors are somewhat suppressed by the factor $q_1^2/(q_1^2 - q_2^2)$]. For example, for $\omega_1 = 8$, $\omega_2 = 16$, $q_1^2/(q_2^2 - q_1^2) = \frac{1}{3}$,

$$\Delta(\omega_1, \omega_2) = (0.6 \pm 0.5) \times 10^{-3} \mu^{-1}.$$

This correction term changes f^2 to

$$f^2 = 0.076 \pm 0.0035.$$

The above method can be applied to the energy-weighted average amplitudes in two energy intervals (a, b) and (c, d) such that (c, d) is far away from (a, b) .

(b) *Reduction of the bound for $|I_A(\omega)|$ by measuring the total cross sections at higher energies.* We recall that the bound for $|I_A(\omega)|$ is $(\mu/N)I_S(\omega)$. For ω fixed, since $I_S(\omega)$ is a decreasing function of N , as we increase the cutoff energy by measuring the total cross sections at higher energy, $(\mu/N)I_S(\omega)$ decreases roughly as $1/N^2$; consequently the bound on $|I_A(\omega)|$ is greatly reduced. For example, at present, $N = 60$ GeV, the bound is $(1.0 \pm 0.2) \times 10^{-3} \mu^{-1}$. With the coming data on total cross sections available up to 300 GeV, the bound will be reduced to $\frac{4}{100} \times (1.0 \pm 0.2) \times 10^{-3} \mu^{-1}$, so that to an accuracy of better than 0.04% one can determine f^2 without any knowledge of the total cross sections beyond 300 GeV. This reduction in principle can be obtained with data on $\pi^{\pm}p$ total cross sections at NAL. In this case one can determine f^2 using the data on $\text{Re}f^{\pm}(\omega)$ in the region 8–20 GeV, by means of the energy-weighted dispersion relation for $f_A(\omega)$, i.e., Eq. (36').

(c) *Reduction of the bound for $|I_A(\omega)|$ by measuring $\text{Re}f^{\pm}(\omega)$ at lower energies.* Instead of increasing N by measuring the total cross sections at higher energies, one can measure $\text{Re}f^{\pm}(\omega)$ at lower energies, below 8 GeV, in order to reduce the bound of $|I_A(\omega)|$. Since $I_S(\omega)$ increases quadratically with ω (approximately), a very large reduction of $|I_A(\omega)|$ is easily obtained. As an example, for ω in the region 4–8 GeV, $|I_A(\omega)| < \frac{1}{4} (1.0 \pm 0.2) \times 10^{-3} \mu^{-1}$ at $\omega = 4$ GeV, while for the averaged dispersion relation

$$\langle \epsilon(\omega_1, \omega_2) \rangle \approx \frac{1}{2} (1.0 \pm 0.2) \times 10^{-3} \mu^{-1},$$

for $\omega_1 = 4$ GeV, $\omega_2 = 8$ GeV.

In summary, better determination of f^2 can be made with future experimental data on $\text{Re}f^{\pm}(\omega)$ in the 4–8-GeV region or with data on total cross sections up to 200–300 GeV.

B. Determination of f^2 and Low-Energy πN Parameters from Low-Energy Data

1. Conventional Method

We now use the bounds for $I_S(\omega)$ and $I_A(\omega)$ given in Eqs. (9) and (14) to analyze the dispersion relations for $f_S(\omega)$ and $f_A(\omega)$ in the low-energy region extended from the threshold to energies below the resonance region in pion-nucleon scattering.¹¹ The application of (9) and (14) to the derivation of the bounds for $\text{Re}f_S(\omega)$ is straightforward. In this energy region, due to the presence of the factor $(q/q_2)^2$, the contribution from $I_S(\omega)$ to the dispersion integral is strongly suppressed and the difference between the lower and upper limits is much reduced; as an example, for $q = 100$ MeV/ c , one gets

$$I_S(\omega) \approx \left(\frac{q}{q_2}\right)^2 I_S(\omega_2) = 0.7 \times 10^{-4} \mu^{-1} (\omega_2 = 20 \text{ GeV}).$$

The lower and upper bounds for $I_S(\omega)$ thus differ by an amount of $0.2 \times 10^{-5} \mu^{-1}$. Neglecting this difference, we have

$$\begin{aligned} Y(\omega) &= \left(\frac{\omega^2}{\mu^2} - \frac{\mu^2}{4M^2}\right) \left[\text{Re} f_S(\omega) - J_S(\omega) - \left(\frac{q}{q_2}\right)^2 I_S(\omega_2) \right] \\ &= - \left[\frac{\mu^2}{4M^2} f_S(\mu) + \frac{f^2}{M} \left(1 - \frac{\mu^2}{4M^2}\right)^{-1} \right] \\ &\quad + \frac{\omega^2}{\mu^2} \left[\frac{f^2}{M} \left(1 - \frac{\mu^2}{4M^2}\right)^{-1} + f_S(\mu) \right]. \end{aligned} \quad (46)$$

The right-hand side of (46) is a linear function of $(\omega/\mu)^2$. A knowledge of $\text{Re} f_S(\omega)$ in the low-energy region will enable us to plot $Y(\omega)$ as a linear function of $(\omega/\mu)^2$, and obtain $f_S(\mu)$ and f^2 . This method in principle provides a reliable determination of $\text{Re} f_S(\mu)$ and f^2 using data on $\text{Re} f_S(\omega)$ at points where $(q/q_2)^2 I_S(\omega_2)$ is much smaller than the right-hand side of (46).

Similarly, for the crossing-odd amplitude $f_A(\omega)$ in the low-energy region, one can write using (5) and neglecting the difference between the lower and upper bounds [ω_2 taken in the region 8–20 GeV where data on $\text{Re} f_A(\omega_2)$ are available] for $|I_A(\omega)|$

$$\begin{aligned} \frac{q^2}{\omega^2 - (\mu^2/2M)^2} \left(\frac{2f^2}{\mu} \right) &= \left(1 - \frac{\mu^2}{4M^2}\right) \left\{ -f_A(\mu) + \frac{\mu}{\omega} \text{Re} f_A(\omega) - J_A(\omega) \right. \\ &\quad \left. + \frac{q^2}{q_2^2 - q^2} \left[\frac{\mu}{\omega} \text{Re} f_A(\omega) - \frac{\mu}{\omega_2} \text{Re} f_A(\omega_2) + J_A(\omega_2) - J_A(\omega) \right] \right\}, \end{aligned} \quad (47)$$

which can also be written in the following form:

$$\begin{aligned} Z(\omega) &= \left(\frac{\omega^2}{\mu^2} - \frac{\mu^2}{4M^2}\right) \left(1 - \frac{\mu^2}{4M^2}\right) \left\{ \frac{\mu}{\omega} \text{Re} f_A(\omega) - J_A(\omega) + \frac{q^2}{q_2^2 - q^2} \left[\frac{\mu}{\omega} \text{Re} f_A(\omega) - \frac{\mu}{\omega_2} \text{Re} f_A(\omega_2) + J_A(\omega_2) - J_A(\omega) \right] \right\} \\ &= - \left\{ f_A(\mu) \left[\left(\frac{\mu^2}{4M^2}\right) \left(1 - \frac{\mu^2}{4M^2}\right) \right] + \frac{2f^2}{\mu} \right\} + \frac{\omega^2}{\mu^2} \left[\frac{2f^2}{\mu} + f_A(\mu) \left(1 - \frac{\mu^2}{4M^2}\right) \right]. \end{aligned} \quad (48)$$

By plotting the experimental values of $Z(\omega)$ as a function of ω^2/μ^2 , one could easily obtain f^2 and $f_A(\mu)$. This, together with the results for f^2 and $f_S(\mu)$, provides a consistent determination of f^2 and the $a_{\pm} \pi^{\pm} p$ s -wave scattering lengths.

2. Direct Determination from Energy-Weighted Average Dispersion Relation

All the remarks concerning the principal-part integration and the energy-weighted average amplitude discussed in previous sections can be straightforwardly applied to the low-energy case. By integrating Eqs. (46) and (48) over an energy interval above the threshold with an appropriate energy weight function $\rho(\omega)$ one gets two equations for f^2 , $f_S(\mu)$, and $f_A(\mu)$ which together with Eq. (39) allow us to determine f^2 and the $\pi^{\pm} N$ s -wave scattering lengths directly from the data on total cross sections in the low- and high-energy regions. For example, taking $\rho(\omega) = 1$, from (46) and (48) one immediately gets

$$\frac{1}{3} \left(1 - \frac{\mu^2}{4M^2}\right)^{-1} \frac{f^2}{M} \left(\frac{\omega_2^2 + \omega_2 \omega_1 + \omega_1^2}{\mu^2}\right) \left[-\frac{\mu^2}{4M^2} f_S(\mu) + \frac{f^2}{M} \left(1 - \frac{\mu^2}{4M^2}\right)^{-1} \right] + \frac{1}{3} f_S(\mu) \left(\frac{\omega_2^2 + \omega_2 \omega_1 + \omega_1^2}{\mu^2}\right) = \langle Y(\omega_1, \omega_2) \rangle, \quad (46')$$

$$- \left\{ \frac{2f^2}{\mu} + f_A(\mu) \left[\frac{\mu^2}{4M^2} \left(1 - \frac{\mu^2}{4M^2}\right) \right] \right\} + \frac{1}{3} \left[\frac{2f^2}{\mu} + f_A(\mu) \left(1 - \frac{\mu^2}{4M^2}\right) \right] \left(\frac{\omega_2^2 + \omega_2 \omega_1 + \omega_1^2}{\mu^2}\right) = \langle Z(\omega_1, \omega_2) \rangle, \quad (48')$$

where

$$\langle Y(\omega_1, \omega_2) \rangle = \left(\frac{1}{\omega_2 - \omega_1}\right) \int_{\omega_1}^{\omega_2} Y(\omega) d\omega,$$

$$\langle Z(\omega_1, \omega_2) \rangle = \left(\frac{1}{\omega_2 - \omega_1}\right) \int_{\omega_1}^{\omega_2} Z(\omega) d\omega.$$

The only unknown quantities in $\langle Y(\omega_1, \omega_2) \rangle$ and $\langle Z(\omega_1, \omega_2) \rangle$ are the data on $\text{Re} f_A(\omega)$ and $\text{Re} f_S(\omega)$ in the low-energy interval (ω_1, ω_2) . These data, once

available at pion factories, will give us immediately the values of f^2 and the scattering lengths a_{\pm} without the usual extrapolations to the threshold.

IV. CONCLUSION

The main results of this work can be summarized as follows:

(1) The experimental data on $\text{Re} f^{\pm}(\omega)$ in the 8–20-GeV region are compatible with the forward dispersion relation. What one learns from this

analysis is that to test the dispersion relation it is necessary to have the total cross sections measured up to energies much higher than the energies at which the real parts are determined.

(2) In the 8–20-GeV region, a more stringent test of the dispersion relation [i.e., an absolute determination of $\text{Re}f_S(\omega)$] requires measurements of the $\pi^\pm p$ total cross sections from 60 to 500 GeV. Conversely, if the dispersion relation is valid, we must have on the average

$$\sigma^+ + \sigma^- \leq 50 \pm 3 \text{ mb}.$$

(3) The experimental values of $\text{Re}f^\pm(\omega)$ in the 8–20-GeV region and the total cross sections up to 60 GeV provide an upper bound for $|I_A(\omega)|$ which allows a determination of f^2 in terms of πN s-wave scattering lengths to an accuracy of better

than 1% without requiring a measurement of the total cross sections beyond 60 GeV. A better determination with greater precision can be made with more data on $\text{Re}f^\pm(\omega)$ at lower energies (in the GeV region) or with data on $\pi^\pm p$ total cross sections beyond 60 GeV.

(4) A test of energy variation of $\text{Re}f_A(\omega)$ and $\text{Re}f^\pm(\omega)$ in the 8–20-GeV region can be done without requiring a precise determination of πN low-energy parameters and the πN coupling constant when data on the total cross sections are available up to 300 GeV.

(5) The πN low-energy parameters can be determined to a great accuracy (without any knowledge of the total cross sections beyond the Serpukhov energy) once the measurements of $\text{Re}f^\pm(\omega)$ are made in the low-energy region.

*Equipe de Recherche Associée au C.N.R.S.

¹M. Froissart, Phys. Rev. **123**, 1053 (1961); A. Martin, Nuovo Cimento **42**, 930 (1966); *ibid.* **44**, 1219 (1966).

²K. J. Foley *et al.*, Phys. Rev. Lett. **19**, 193 (1967).

³After completing this work we became aware that inequality (9) has been previously derived by B. Lautrup, P. Møller Nielsen, and P. Olesen, Phys. Rev. **140**, 984 (1965).

⁴Data on $\pi^\pm p$ total cross sections are taken from: V. S. Barashenkov, *Interaction Cross Sections of Elementary Particles* (Israel Program for Scientific Translation, Jerusalem, 1968); A. A. Carter *et al.*, Nucl. Phys. **B26**, 445 (1971); A. A. Carter *et al.*, Phys. Rev. **168**, 1457 (1968); A. Citron *et al.*, Phys. Rev. **144**, 1101 (1966); K. J. Foley *et al.*, Phys. Rev. Lett. **19**, 330 (1967); S. P. Denisov *et al.*, Phys. Lett. **36B**, 415 (1971).

⁵N. Khuri and T. Kinoshita, Phys. Rev. Lett. **14**, 84 (1965); A. Martin, Phys. Lett. **15**, 76 (1965).

⁶M. L. Goldberger, H. Miyazama, and R. Oehme, Phys. Rev. **99**, 986 (1955).

⁷G. Höhler and R. Strauss, Z. Phys. **240**, 377 (1970).

⁸J. Hamilton, Phys. Lett. **20**, 687 (1966).

⁹J. Hamilton and W. S. Woolcock, Rev. Mod. Phys. **35**, 737 (1963).

¹⁰V. K. Samaranayake and W. S. Woolcock, Nucl. Phys.

B48, 205 (1972), and references to previous works cited therein.

¹¹See Refs. 7 and 10 for previous works on the subject. In particular, this work differs essentially from that of Höhler and Strauss (Ref. 7) in the way of handling the high-energy integrals: Instead of using a parametrization of the total cross sections beyond 60 GeV, we use the data on the real parts of Foley *et al.* to deduce a bound on $I_S(\omega)$ and $I_A(\omega)$. It should be pointed out here that our results confirm the small value for $I_A(\omega)$ computed with a Regge-pole model used in Refs. 9 and 10.